Biomass-Based Leaf Curvilinear Model for Rapeseed (*Brassica napus* L.)

Wenyu Zhang, Weixin Zhang, Daokuo Ge, Hongxin Cao(✉), Yan Liu, Kunya Fu, Chunhuan Feng, Weitao Chen, and Chuwei Song

Institute of Agricultural Economics and Information/Engineering Research Center for Digital Agriculture, Jiangsu Academy of Agricultural Sciences, Nanjing 210014, China
research@wwery.cn, nkyzwx@126.com, gedakuo@163.com, caohongxin@hotmail.com, liuyan0203@aliyun.com, 921186907@qq.com, 1286234727@qq.com, 1303079141@qq.com, 923903764@qq.com

Abstract. Leaf is one of the most important photosynthetic organs of rapeseed (*Brassica napus* L.). To quantify relationships between the leaf curve and the corresponding leaf biomass for rapeseed on main stem, this paper presents a biomass-based leaf curvilinear model for rapeseed. Various model variables, including leaf length, bowstring length, tangential angle, and bowstring angle, were parameterized based on data derived from the field experiments with varieties, fertilizer, and transplanting densities during 2011 to 2012, and 2012 to 2013 growing seasons. And then we analysed the biological significance of curvilinear equation for straight leaves, constructed the straight leaf probabilistic model on main stem, quantified the relationship between leaf curvature and the corresponding leaf biomass, and constructed the leaf curvilinear model based on the assumption and verification of the curvilinear equation form for curving leaf. The probability of straight leaf can be quantified with piecewise function according to the different trend in the normalized leaf ranks ((0, 0.4], and (0.4, 1]). The leaf curvature decreased with the increasing of leaf biomass, and can be described with reciprocal function. The curve of straight leaf and the curving leaf can be simulated by linear equation and the quadratic function, respectively. Our models were validated with the independent dataset from the field experiment, and the results indicated that the model could effectively predict the straight leaf probability and leaf curvature, which would be useful for linking the rapeseed growth model with the rapeseed morphological model, and set the stage for the development of functional-structural rapeseed models.

Keywords: Rapeseed (*Brassica napus* L.) · Biomass · Leaf curve · Functional-structural plant models (FSPMs)

1 Introduction

Rapeseed is the world's important oil crops [1] with harvest area of 25.3 to 30.9 million ha and total yield of 46.5 ~ 72.5 million tons during 2004 ~ 2013 [2]. At the same time, it is the main oilseed crop in China [3], whose harvest area is about 5.6 ~ 7.5 million ha,

D. Li and Z. Li (Eds.): CCTA 2015, Part I, IFIP AICT 478, pp. 459–472, 2016.
DOI: 10.1007/978-3-319-48357-3_44

and the total yield is about 10.6 ~ 14.4 million tons [2] in general. Also, it is one of the main raw material of biodiesel [4]. Therefore, it is very important for ensure food and ecological security that promote the development of rapeseed production.

Light distribution characteristics in crop canopies directly affect the light energy utilization efficiency for photosynthesis, dry matter accumulation, and yield formation. All most all the growth models predicted the crop canopy light distribution through the Beer's law [5–8], in that the two key factors for light distribution simulation process, the extinction coefficient and the layered leaf area index, are closely related with the leaf curving characteristics [9]. Therefore, quantitatively modeling of the leaf curve could provide a mechanistic way for precisely simulating the crop canopy structure, light distribution, and photosynthesis, and lay a foundation for the predicting of light energy utilization efficiency and yield formation.

At present, there are many studies on leaf curve modeling. In the study of mathematical characterization of maize canopies [10], leaf curve was described as a general quadratic equation expressed by the initial leaf angle, the coordinates of the leaf tip and the leaf's maximum height. The general quadratic equation was also used to simulate the leaf curve of maize [11–13], rice [14], and other crops by many researchers. Leaf curve was also fitted into a quadratic function for rice [15, 16] and winter wheat [17], or a Gaussian function for spring barley [18] and rice [19]. Furthermore, Espana et al. [20] decomposed leaf curvature into two parts, the ascending part was described as a parabolic curve, and the descending part, when existing, was characterized by a portion of an ellipse, and then applied the leaf curvature model to maize canopy 3D architecture and reflectance simulation. Watanabe et al. [21] found that leaf curves could be fitted using Hermite functions though analyzing three angles related to the basal, mid, and tip of leaf. Shi et al. [22] characterized the rice leaf curve by a second order differential equation, including the synthetic effect of leaf blade length, width, specific leaf weight, initial leaf angle, and the deformation coefficient on leaf space shape, using force analyzing on rice leaf. Zheng et al. [23] obtain leaf midrib coordinate points by cubic spatial B-spline interpolation, and characterized the leaf curves as the connecting line of these points.

It is difficult to measure leaf curve because of the intricate leaf shape for rapeseed. Therefore, the objectives of this research were to develop straight leaf probabilistic model, straight leaf curvilinear model, and biomass-based leaf curvilinear model by linking leaf morphological parameters with the corresponding leaf biomass, to validate the hypothesis that the curvilinear function for curving leaves could be fitted as quadratic function, and to provide a reference for linking morphological parameters with corresponding organ biomass, and for the establishment of the FSPMs.

2 Materials and Methods

2.1 Materials

We used 2 rapeseed cultivars, they are: "Ningyou 18" (V1, conventional), and "Ningza 19" (V2, hybrid), breed by Institute of Economic Crops Research, Jiangsu Academy of Agricultural Sciences.

2.2 Methods

2.2.1 Experimental Conditions and Design

In order to determine the parameters and verify the models, three experiments were conducted involving different varieties, transplanting densities, and fertilizer during the 2011–2012, and 2012–2013 growing seasons at the experimental farm of our Academy (32.03°N, 118.87°E). The soil type is a hydragric anthrosol (organic carbon, 31.4 g kg^{-1}; total nitrogen, 2.03 g kg^{-1}; available phosphorus, 20.3 mg kg^{-1}; available potassium, 139.0 mg kg^{-1}; and pH 7.31).

Exp. 1, variety and the fertilizer experiment (2011–2012): The Experiment was deployed in split block design with three replications. Two fertilizer levels (N0 = no fertilizer; N2 = 180 kg ha^{-1}) were the whole-plot treatments while two cultivars (V1 and V2) constituted the sub-plots. The plots arranged random with 0.4 m row spacing, 0.17–0.20 m plant spacing in 7.0 × 5.7 m area. Fertilizer contained 12 kg P_2O_5 ha^{-1},18 kg K_2O ha^{-1}, and 15 kg boron ha^{-1}.

Exp. 2, variety experiment (2012–2013): The experiment was deployed in randomized complete block design with 2 varieties (V1 and V2) and 3 replications. Nitrogen fertilizer included 90 kg N ha^{-1}(N1), and the transplanting density was 1.2×10^5 plant ha^{-1}(D2).

Exp. 3, variety, fertilizer and transplanting density experiment (2012–2013): The Experiment was deployed in split block design with three replications. Three fertilizer levels (N0 = no fertilizer; N1 = 90 kg ha^{-1}; N2 = 180 kg ha^{-1}) were the whole-plot treatments while variety (V1) and three transplanting densities (D1 = 6×10^4 plant ha^{-1}; D2 = 1.2×10^5 plant ha^{-1}; D3 = 1.8×10^5 plant ha^{-1}) constituted the sub-plots.

The plots of Exp. 2 and Exp. 3 arranged random with 0.42 m row spacing in 3.99 by 3.5 m area, and the plant spacing was calculated by row spacing and transplanting density. Fertilizer contained 90 kg P_2O_5 ha^{-1} and 90 kg K_2O ha^{-1} for N1 plots, and 180 kg P_2O_5 ha^{-1} and 180 kg K_2O ha^{-1} for N2 plots, and 15 kgboron ha^{-1} was used as foliage spray for both N1 and N2 plots after bolting.

2.2.2 Measurements

The leaf rank on the main stem of 50 randomly selected seedlings for each plot were marked using a red number stamp before transplanting. Leaf morphological parameters including leaf length (the distance between leaf basal and leaf tip in the straight state, including the leaf blade and petiole, if it exists. *LL*, for short), leaf tangential angle (the angle between the tangential direction of leaf basal and the main stem. *TA*, for short), leaf bowstring angle (the angle between the straight line from leaf basal to leaf tip in natural state and the main stem. *BA*, for short), and leaf bowstring length (the distance between leaf basal and leaf tip in natural state. *LBL*, for short) were measured using straightedge and protractor directly (Fig. 1).

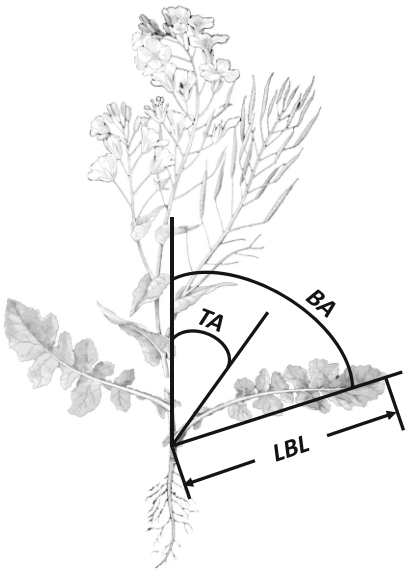

Fig. 1. Diagram of *TA*, *BA* and *LBL*

2.2.3 Data Analysis

We wrote a C# Program to solve the approximate solution of leaf curve equation parameters through a step of 10^{-5} cm. Leaf rank data were normalized to (0, 1] interval, in order to eliminate the apparent differences between treatments and replications. The data from Exp. 1 was used for model development, data from Exp. 2, and Exp. 3 were used for validation.

2.2.4 Model Validation

We validated the models developed in this paper by calculating the correlation (r), the root mean square error (*RMSE*), the average absolute difference (d_a), and the ratio of d_a to the average observation (d_{ap}) [24], and 1:1 line of simulated and observed properties. Some statistical indices were defined as follows:

$$RMSE = \sqrt{\frac{\sum_{i=1}^{n}(O_i - S_i)^2}{n}}$$

$$d_a = \frac{1}{n}\sum_{i=1}^{n}(O_i - S_i)$$

$$d_{ap}(\%) = |d_a|/\bar{O} \times 100$$

where i is sample number, n is total number of measurements, $n - 1 = n$ when $n \geq 30$, S_i is simulated value, and O_i is observed value.

3 Results

3.1 Model Description

3.1.1 Probability and Curvilinear Model for Straight Leaves

In order to represent the extension state of leaf better, we set the leaf in the Cartesian coordinate system with the leaf basal point as the origin and growth direction of main stem as y-axis, regardless of leaf distorting. According to observations in the Exp. 1, some rapeseed leaves could be considered as straight leaves with small difference between leaf length and leaf bowstring length, as well as leaf tangential angle and leaf bowstring angle. Therefore, we treated the leaves as straight leaves if difference between the leaf length and the leaf bowstring length was less than 1 cm or difference between the leaf tangential angle and the leaf bowstring angle is less than 10°. The curvilinear equation ($f(x)$) of straight leaves could be expressed as a linear function which passes through the origin and with the cotangent value of the leaf tangential angle as the slope, and the function could be described by Eq. (1).

$$f(x) = \cot(TA) \cdot x \tag{1}$$

where TA can be simulated by our previous model [25].

The data in the Exp. 1 showed that changes in the probability of different treatments for straight leaves by the normalized leaf ranks was close to quadratic curve with significant r ($r = 0.725$, $P < 0.01$, $n = 16$, $r_{(14,\ 0.01)} = 0.623$, Table 1) in the interval (0, 0.4] (Fig. 2a), and logarithmic curve with significant r ($r = 0.925$, $P < 0.001$, $n = 33$, $r_{(31,\ 0.001)} = 0.547$, Table 1) in the interval (0.4, 1] (Fig. 2b). So that the probability of straight leaves by the normalized leaf ranks (P_{LS}) could be expressed as a piecewise function as Eq. 2.

$$P_{LS} = \begin{cases} A_1 \cdot NLRs^2 + B_1 \cdot NLRs + C_1 & NLRs \in (0, 0.4] \\ A_2 \cdot \ln(NLRs) + B_2 & NLRs \in (0.4, 1] \end{cases} \tag{2}$$

where $NLRs$ is normalized leaf rank; A_1, A_2, B_1, B_2, and C_1 are model parameters whose values and testing data shown in Table 1.

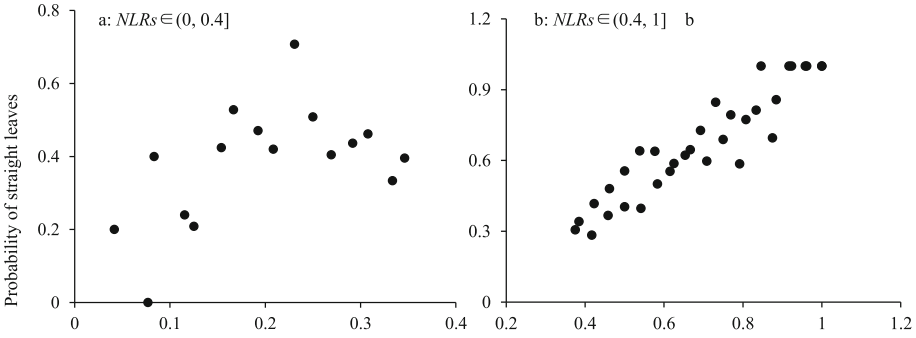

Fig. 2. Changes in the probability of straight leaves with the normalized leaf ranks

Table 1. Significance test of the straight leaf probabilistic model and its parameters

Interval of normalized leaf ranks	Function	n	r	Sig. for r	Sig. for F	Parameter symbolic	Unstandardized coefficients	t
(0, 0.4]	$A_1 \cdot NLRs^2 + B_1 \cdot NLRs + C_1$	16	0.725^{**}	$r_{(14,\ 0.01)} = 0.623$	0.008	A_1	−10.519	-2.709^{*}
						B_1	1.572	3.199^{**}
						C_1	0.139	−0.800
(0.4, 1]	$A_2 \cdot \ln(NLRs) + B_2$	33	0.925^{***}	$r_{(31,\ 0.001)} = 0.547$	0.000	A_2	0.716	13.575^{***}
						B_2	0.965	36.223^{***}

***, **, and * denote significance at $P < 0.001$, $P < 0.01$, and $P < 0.05$, respectively. The same as below.

3.1.2 Curvilinear Model for Curving Leaves

3.1.2.1 Assumed Functions and There Biological Significance for Leaf Curve

According to the leaves curving characteristics observed in experiments, and the research on curvilinear models for other crops, we supposed that curvilinear function of rapeseed leaf ($f(x)$) could be fitted by functions such as quadratic function ($ax^2 + bx$), quartic function ($ax^4 + bx^3 + cx^2 + dx$), sine function ($a\sin(bx)$), Hoerl-like function (axb^x), $(a + bx^c)/(d + x^c)$, and $(a + bx)/(1 + cx + dx^2)$, whose diagram were similar to leaf curves in a interval. On the basis of geometric meaning of derivative, $\cot(TA)$ can be interpreted as $f'(0)$ (value of leaf curvilinear equation's derived function at origin of coordinates), thus, biological significance of leaf curvilinear equation parameters are showed in Table 2.

Table 2. The various functions of leaf curve, their derivative function and the derivative value at the origin, and the biological significance of the parameters

$f(x)$	$f'(x)$	$f'(0)$	Biological significance of the parameters
$ax^2 + bx$	$2ax + b$	b	$-a$: curvature; $b = \cot(TA)$
$ax^4 + bx^3 + cx^2 + dx$	$4ax^3 + 3bx^2 + 2cx + d$	d	$d = \cot(TA)$
$a\sin(bx)$	$ab\cos(bx)$	ab	leaf curve peak: $(\pi/2b, a)$; $ab = \cot(TA)$
axb^x	$ab^x\log(b)x + ab^x$	a	$a = \cot(TA)$; $-b$: curvature
$(a + bx^c)/(d + x^c)$	$\frac{bcx^{c-1}}{x^c+d} - \frac{cx^{c-1}(bx^c+a)}{(x^c+d)^2}$	0	N/A
$(a + bx)/$ $(1 + cx + dx^2)$	$\frac{b}{dx^2+cx+1} - \frac{(bx+a)(2dx+c)}{(dx^2+cx+1)^2}$	b $-ac$	$b-ac = \cot(TA)$

From Table 2, we saw that only quadratic function, sine function, and Hoerl-like function had specific biological significance for all the parameters: for quadratic function $ax^2 + bx$, $-a$ expresses the leaf curvature, and b expresses the cotangent value of leaf tangential angle; for sine function $a\sin(bx)$, a expresses the ordinate value of leaf curve peak point, $\pi/2b$ abscissa value of expresses the leaf curve peak point, and ab expresses the cotangent value of leaf tangential angle; for Hoerl-like function axb^x, a expresses the cotangent value of leaf tangential angle, and $-b$ expresses the leaf curvature. So that we addressed them and validated the assumptions.

3.1.2.2 Solution of the Leaf Curvilinear Equation

As shown in Fig. 3, the leaf tip could be expressed as (sin (*BA*)•*LBL*, cos(*BA*)•*LBL*) by solving $\Delta OL_t y_t$. We substituted coordinates of origin and L_t into curvilinear function for curving leaves to get equation set as Eq. 3.

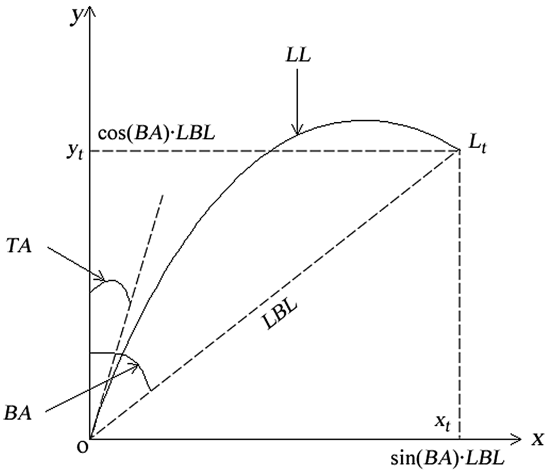

Fig. 3. The geometrical properties of leaf curve

$$\begin{cases} f(\sin(BA)\cdot LBL) = \cos(BA)\cdot LBL \\ f'(0) = \cot(TA) \end{cases} \tag{3}$$

The equation sets and their solutions corresponding to the three curvilinear functions for curving leaves we supposed above were shown in Table 3.

Table 3. Three curvilinear functions for curving leaves and the corresponding equation sets and their solutions

f(*x*)	Equation set	Solution
$ax^2 + bx$	$\begin{cases} f(\sin(BA)\cdot LBL) = a\cdot\sin(BA)^2\cdot LBL^2 + b\cdot LBL\cdot\sin(BA) = \cos(BA)\cdot LBL \\ f'(0) = b = \cot(TA) \end{cases}$	$a = -\frac{\sin(BA)\cdot\cot(TA)-\cos(BA)}{LBL\cdot\sin(BA)^2}b = \cot(TA)$
$a\sin(bx)$	$\begin{cases} f(\sin(BA)\cdot LBL) = a\cdot\sin(b\cdot LBL\cdot\sin(BA)) = \cos(BA)\cdot LBL \\ f'(0) = a\cdot b = cot(TA) \end{cases}$	$a = \frac{LBL\cdot\cos(BA)}{\sin(b\cdot LBL\cdot\sin(BA))}$ $a\cdot b = \cot(TA)$
axb^x	$\begin{cases} f(\sin(BA)\cdot LBL) = a\cdot LBL\cdot\sin(BA)\cdot b^{LBL\cdot\sin(BA)} = \cos(BA)\cdot LBL \\ f'(0) = a = \cot(TA) \end{cases}$	$a = \cot(TA)$ $b = \left(\frac{cos(BA)}{\sin(\sin(BA)\cdot\sin(TA))}\right)^{\frac{1}{\sin(BA)\cdot LBL}}$

As shown in Table 3, quadratic function, and Hoerl-like function could be solved directly, but there was no analytical solution for sine function, and we wrote a C# program to calculate the approximate solution with a step of 10^{-5} cm.

3.1.2.3 Validation for Leaf Curvilinear Functions

We used the observed value of tangential angle, bowstring angle, and bowstring length for solving equation set, except leaf length. Meanwhile, the leaf length also could be calculated as the arc length between leaf basal and leaf tip by the formula of arc length. Therefore, we can validate the leaf curvilinear functions through comparing the observed leaf length with the calculated arc length. The three leaf curvilinear functions were validated by 1:1 line of observed and calculated leaf length (Fig. 4), and the statistical parameters were shown in Table 4.

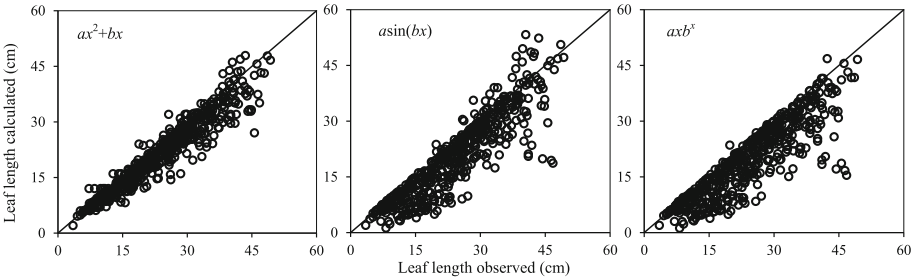

Fig. 4. Comparison of the observed and the stimulated leaf length on main stem in 2011–2012

Table 4. Comparison of statistical parameters of the observed and the stimulated leaf blade length on main stem in 2011–2012

$f(x)$	Statistic parameters of simulation and observation					
	n	d_a(cm)	d_{ap}(%)	$RMSE$(cm)	r	Sig.
$ax^2 + bx$	509	2.521	10.426	3.974	0.956^{***}	$r_{(507,0.001)} = 0.145$
$a\sin(bx)$	509	3.730	15.427	6.083	0.904^{***}	$r_{(507,0.001)} = 0.145$
axb^x	509	4.693	19.410	6.749	0.889^{***}	$r_{(507,0.001)} = 0.145$

The results showed that the best fitted one (with the highest r and lowest d_a,d_{ap}, and $RMSE$, Table 4) with specific biological significance (Table 2) for leaf curve was quadratic function, so that the curvilinear model for curving leaves could be described as a quadratic function as Eq. (4).

$$f(x) = -Lc_i \cdot x^2 + \cot(TA) \cdot x \tag{4}$$

where, Lc_i is the leaf curvature on the ith day after emergence.

3.1.2.4 Biomass-Based Leaf Curvature Simulation

The data in the experiments showed that quadratic coefficients of leaf curvilinear equations increased with the increase of corresponding leaf dry weight from leaf fully

expanded until senescence. It means that leaf curvature decreased with the corresponding leaf biomass (Fig. 5), and could by fitted by reciprocal function with significant r (V1: $r = 0.974$, $P < 0.001$, $n = 34$, $r_{(32,\ 0.001)} = 0.539$; V2: $r = 0.637$, $P < 0.001$, $n = 51$, $r_{(49,\ 0.001)} = 0.447$. Table 5).

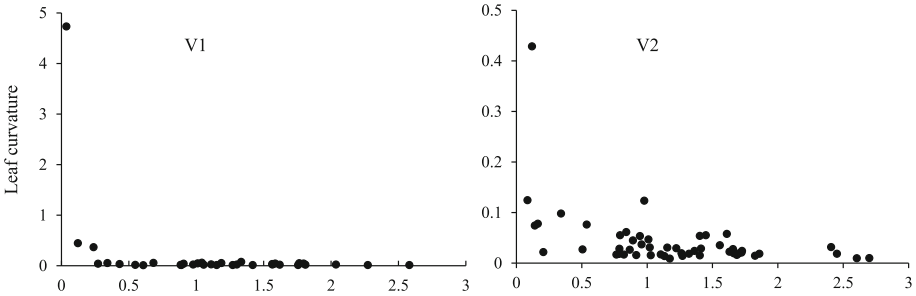

Fig. 5. Changes in the leaf curvature with the leaf dry weight in 2011–2012

Table 5. Significance test of the leaf curvature model and its parameter

Cultivar	n	r	Sig. for r	Sig. for F	Parameter symbolic	Unstandardized coefficients	t
V1	34	0.974^{***}	$r_{(32,\ 0.001)} = 0.539$	0.000	Lc_a	−0.165	-24.127^{***}
					Lc_b	0.163	4.625^{***}
V2	51	0.637^{***}	$r_{(49,\ 0.001)} = 0.447$	0.000	Lc_a	−0.018	-5.789^{***}
					Lc_b	−0.015	−1.826

$$Lc_i = \frac{-Lc_a}{DWLB_i} - Lc_b \tag{5}$$

where $DWLB_i$ is the dry weight on the ith day after emergence; Lc_a and Lc_b are model parameters whose values and testing data shown in Table 5.

3.2 Validation

The models developed above were validated were validated with the independent datasets from Exp. 2 and Exp. 3, and the results showed that the correlation (r) of simulation and observation probability for straight leaves and curvature for curving leaves all had significant level at $P < 0.001$, and that the average absolute difference (d_a), the ratio of d_a to the average observation (d_{ap}), and the root mean square error ($RMSE$) all were smaller (Table 6). Figures 6 and 7 indicated that the observed and simulated probability for straight leaves and curvature for curving leaves were all close to the 1:1 line.

Table 6. Comparison of statistical parameters of simulation and observation in the probability for straight leaves and curvature for curving leaves on main stem in 2012–2013

Models	Cultivar	Statistic parameters of simulation and observation					
		n	d_a	d_{ap}(%)	*RMSE*	*r*	Sig.
Probability for straight leaves	V1, V2	52	0.001	0.245	0.191	0.762***	$r_{(50,0.001)} = 0.443$
Curvature for curving leaves	V1	93	0.007	−9.196	0.060	0.648***	$r_{(91,0.001)} = 0.336$
	V2	99	−0.005	−7.000	0.042	0.541***	$r_{(97,0.001)} = 0.326$

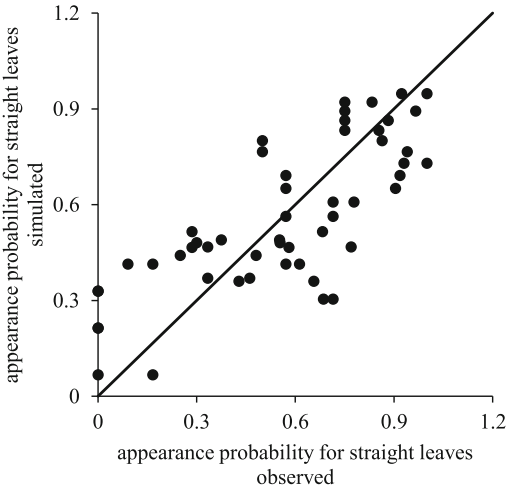

Fig. 6. Comparison of the observed and the stimulated probability for straight leaves in 2012–2013

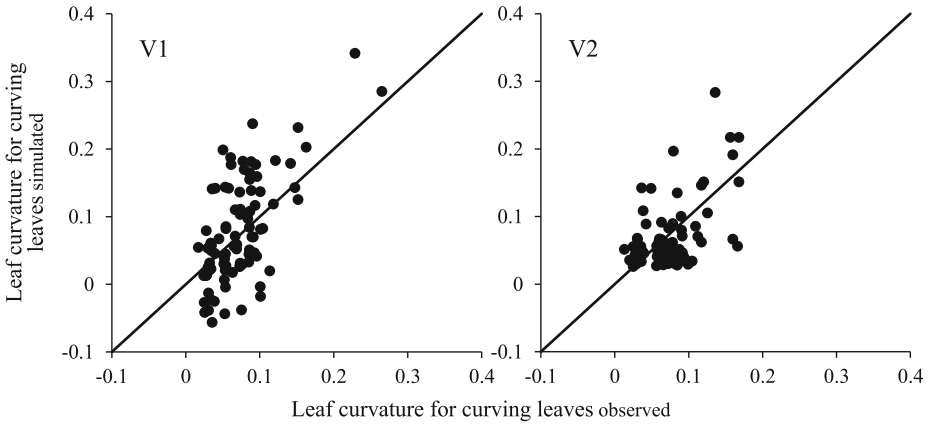

Fig. 7. Comparison of the observed and the stimulated leaf curvature for curving leaves in 2012–2013

4 Discussion

4.1 Establishment of Biomass-Based Leaf Curvilinear Model will Helps to Develop FSRM

Functional-structural plant model with better mechanistic embodies the interaction between plant morphogenesis and cultivars and environmental factors by integrated the functions of growth model with the structures of morphological model [26]. So far, there were lot of research on modeling the leaf curve [10–21] which aimed at 3D reconstruction of crop canopy with a high precision. They well explained the effects of structures on functions by combining technical instrumentalities like geometrical ray trace [27, 28], but could not change the structures as a response of the changed functions. Shi et al. [22] linked leaf curve with corresponding dry weight through force analyzing on rice leaf, but the leaf curvilinear equation which was limited by a form of second order differential equation in this research was difficult to use. Groer et al. [29] established a dynamic 3D model of rapeseed using the modelling language XL [30] and made the morphological model response of different nitrogen levels using a sinks and sources system like GREENLAB and the LEAFC3-N model [31] for photosynthesis at different N-regimes. But the time from sowing to the rosette stage and the conditions except nitrogen was neglected in this model. Jullien et al. [32] constructed a FSPM by characterizing the interactions between architecture and source-sink relationships in winter oilseed rape using the GREENLAB model. However, it mainly considered the relationship between biomass and leaf area [33], and the description of blade shape was relatively simple. Cao et al. [34] and Zhang et al. [25] established models to meticulous predict leaf morphological parameters like leaf length, width, and angles, apart from leaf curve. We developed biomass-based leaf curvilinear model for rapeseed by linking the leaf curvature with the corresponding leaf biomass, which could realize combination of structures with functions, explained effects of environmental conditions on leaf morphogenesis, and set the stage for the development of functional-structural rapeseed models.

4.2 The Research Provided a Mechanistic and Universal Method for Leaf Curve Modeling

As to facilitate observation and simulation, we set the leaf into a Cartesian coordinate system with the leaf basal point as the origin and growth direction of main stem as y-axis. To make the model more precisely, two cases of curving characteristic (straight or curving) were analyzed. In order to determining the form of leaf curvilinear equation to be difficult to measure directly, we compared various functions based on their biological significance, and calculated and observed leaf length. For eliminating the apparent differences between treatments and replications, we normalized the leaf rank into the interval of (0, 1]. All these practices made the model to have better mechanistic and universal.

4.3 Models Developed in This Paper Needs to Be Improved

The biomass-based rapeseed leaf curvilinear model developed in this paper for the stage from leaf fully expanded until senescence, but the processes of leaf extension, senescence, and distorting is neglected. Thus, it needs to be studied further.

5 Conclusions

This paper presents a biomass-based leaf curvilinear model for rapeseed designed to explain effects of cultivars and environmental conditions on leaf curve. Various model variables, including leaf biomass, length, and angles were parameterized based on datasets derived from the experiments with rapeseed cv. Ningyou 18, and Ningza 19.

With the help of our descriptive model, it will be easy to fulfill calculation of leaf curve via biomass, canopy structure via leaf curve, light distribution and the photosynthesis via canopy structure, and biomass via photosynthesis. It should be possible to connection morphological model with physiological model via biomass, and to development the FSRM.

A similar method could also be applied in other crops like maize and rice, and it could help to the regulation and selection for ideal plant type in the future.

Acknowledgments. This work is supported by the grants from the National Natural Science Foundation of China (31171455, 31201127, and 31471415), the National High-Tech Research and Development Program of China (2013AA102305-1), the Jiangsu Agriculture Science and Technology Innovation Fund of China [CX(12)5060], and Jiangsu Academy of Agricultural Sciences Basic Scientific Research Work Special Fund [ZX(15)2008, ZX(15)4001].

References

1. Cao, H., Zhang, C., Li, G., et al.: Researches of optimum shoot and ramification number dynamic models for rapeseed (*Brassica napus* L.). In: World Automation Congress (WAC), pp. 129–135. IEEE (2010)
2. FAO Statistics Division. FAOSTAT [DB/OL] (2015). http://faostat.fao.org/
3. Cao, H., Zhang, C., Li, G., et al.: Researches of optimum leaf area index dynamic models for rape (*Brassica napus* L.). In: Zhao, C., Li, D. (eds.) Computer and Computing Technologies in Agriculture II, Volume 3. IFIP AICT, vol. 295, pp. 1585–1594. Springer, New York (2009)
4. Hama, S., Kondo, A.: Enzymatic biodiesel production: an overview of potential feed stocks and process development. Bioresour. Technol. **135**(2), 386–395 (2013)
5. Kropff, M.J., Laar, H.H.V., Matthews, R.B.: ORYZA1: an ecophysiological model for irrigated rice production. In: SARP Research Proceedings, p. 1994 (1994)
6. Boote, K.J., Pickering, N.B.: Modeling photosynthesis of row crop canopies. HortScience **29** (12), 1423–1434 (1994)
7. Gao, L., Jin, Z., Zheng, G., et al.: Wheat cultivational simulation-optimization-decision making system (WCSODS). Jiangsu J. Agric. Sci. **16**(02), 65–72 (2000). (in Chinese)

8. Tang, L., Zhu, Y., Hannaway, D., et al.: RiceGrow: a rice growth and productivity model. NJAS - Wageningen J. Life Sci. **57**(1), 83–92 (2009)
9. Wang, W., Li, Z., Su, H.: Comparison of leaf angle distribution functions: effects on extinction coefficient and fraction of sunlit foliage. Agric. For. Meteorol. **143**(1–2), 106–122 (2007)
10. Stewart, D.W., Dwyer, L.M.: Mathematical characterization of maize canopies. Agric. For. Meteorol. **66**(3–4), 247–265 (1993)
11. Guo, Y., Li, B.: Mathematical description and three-dimensional reconstruction of maize canopy. Chin. J. Appl. Ecol. **10**(01), 39–41 (1999). (in Chinese)
12. Zhao, C., Zheng, W., Guo, X., et al.: The computer simulation of maize leaf. J. Biomath. **19** (04), 493–496 (2004). (in Chinese)
13. Zheng, W., Guo, X., Zhao, C., et al.: Geometry modeling of maize leaf canopy. Trans. CSAE **20**(01), 152–154 (2004). (in Chinese)
14. Liu, H., Wu, B., Zhang, H., et al.: Research on rice leaf geometric model and its visualization. Comput. Eng. **35**(23), 263–264+268 (2009). (in Chinese)
15. Yang, H., Luo, W., He, H., et al.: 3D morphology modeling and computer simulation of rice main stem. Acta Agriculturae Universitis Jiangxiensis **30**(06), 1153–1156+1160 (2008). (in Chinese)
16. Luo, W., Yang, H., Deng, S., et al.: A study based on multi-segment and proportion geometrical model of rice leaf and 3D morphology modeling. Acta Agriculturae Universitis Jiangxiensis **31**(05), 970–974 (2009). (in Chinese)
17. Chen, G.: Studies on Simulation and Visualization of Morphogenesis in Wheat. Nanjing Agricultural University, Nanjing (2004). (in Chinese)
18. Dornbusch, T., Wernecke, P., Diepenbrock, W.: Description and visualization of graminaceous plants with an organ-based 3D architectural model, exemplified for spring barley (Hordeumvulgare L.). Vis. Comput. **23**(8), 569–581 (2007)
19. Zhang, Y., Tang, L., Liu, X., et al.: Dynamic simulation of leaf curve in rice based on Gaussian function. Sci. Agric. Sin. **46**(01), 215–224 (2013). (in Chinese)
20. España, M.L., Baret, F., Aries, F., et al.: Modeling maize canopy 3D architecture: application to reflectance simulation. Ecol. Model. **122**(1–2), 25–43 (1999)
21. Watanabe, T., Hanan, J.S., Room, P.M., et al.: Rice morphogenesis and plant architecture: measurement, specification and the reconstruction of structural development by 3D architectural modelling. Ann. Bot. **95**(7), 1131–1143 (2005)
22. Shi, C., Zhu, Y., Cao, W.: A quantitative analysis on leaf curvature characteristics in rice. Acta Agron. Sin. **32**(05), 656–660 (2006). (in Chinese)
23. Zheng, B., Shi, L., Ma, Y., et al.: Three-dimensional digitization in situ of rice canopies and virtual stratified-clipping method. Sci. Agric. Sin. **42**(04), 1181–1189 (2009). (in Chinese)
24. Cao, H., Hanan, J.S., Liu, Y., et al.: Comparison of crop model validation methods. J. Integr. Agric. **11**(8), 1274–1285 (2012)
25. Zhang, W., Cao, H., Zhu, Y., et al.: Morphological structure model of leaf space based on biomass at pre-overwintering stage in rapeseed (*Brassica napus* L.) plant. Acta Agron. Sin. **41**(02), 318–328 (2015). (in Chinese)
26. Cao, H., Zhao, S., Ge, D., et al.: Discussion on development of crop models. Sci. Agric. Sin. **44**, 3520–3528 (2011). (in Chinese)
27. Chelle, M., Saint-Jean, S.: Taking into account the 3D canopy structure to study the physical environment of plants: the Monte Carlo solution. In: 4th International Workshop on Functional-Structural Plant Models, pp. 176–180 (2004)
28. Ma, Y., Wen, M., Li, B., et al.: Efficient model for computing the distribution of direct solar radiation in maize canopy at organ level. Trans. CSAE **23**(10), 151–155 (2007). (in Chinese)

29. Groer, C., Kniemeyer, O., Hemmerling, R., et al.: A dynamic 3D model of rape (Brassica napus L.) computing yield components under variable nitrogen fertilization regimes. In: 5th International Workshop on Functional-Structural Plant Models, pp. 4.1–4.3, November 2007
30. Kniemeyer, O.: Rule-based modelling with the XL/GroIMP software. In: Proceedings of 6th GWAL, pp. 56–65, 14–16 April 2004
31. Müller, J., Wernecke, P., Diepenbrock, W.: LEAFC3-N: a nitrogen-sensitive extension of the CO2 and H2O gas exchange model LEAFC3 parameterised and tested for winter wheat (Triticumaestivum L.). Ecol. Model. **183**, 183–210 (2005)
32. Jullien, A., Mathieu, A., Allirand, J.-M., et al.: Characterization of the interactions between architecture and source-sink relationships in winter oilseed rape (*Brassica napus*) using the GreenLab model. Ann. Bot. **107**(5), 765–779 (2011)
33. Jullien, A., Allirand, J.-M., Mathieu, A., et al.: Variations in leaf mass per area according to N nutrition, plant age, and leaf position reflect ontogenetic plasticity in winter oilseed rape (Brassica napus L.). Field Crops Res. **114**(2), 188–197 (2009)
34. Cao, H., Zhang, W., Zhang, W., et al.: Biomass-based rapeseed (*Brassica napus* L.) leaf geometric parameter model. In: Proceedings of the 7th International Conference on Functional-Structural Plant Models, p. 26, 9–14 June 2013